Galvanic interpretation of self-potential signals associated with microbial sulfate-reduction

Kenneth H. Williams[1,2*], *Susan S. Hubbard*[2] *and Jillian F. Banfield*[1,2]

[1]Department of Environmental Science, Policy & Management, University of California, Berkeley, CA 94720

[2]Lawrence Berkeley National Laboratory, Berkeley, CA 94720

[*]Corresponding author e-mail: khwilliams@lbl.gov; phone: (510) 701-1089

Abstract

We have evaluated the usefulness of the self-potential (SP) geophysical method to track the onset and location of microbial sulfate-reduction in saturated sediments during organic carbon amendment. Following stimulation of sulfate-reducing bacteria (SRB) by addition of lactate, anomalous voltages exceeding 600 mV correlated in space and time with the accumulation of dissolved sulfide. Abiotic experiments in which the sulfide concentration at the measurement electrode was systematically varied showed a positive correlation between the magnitude of the SP anomaly and differences in the half-cell potential associated with the measurement and reference electrodes. Thus, we infer that the SP anomalies resulted from electrochemical differences that developed between sulfide-rich regions and areas having higher oxidation potential. In neither experiment did generation of an SP anomaly require the presence of an *in situ* electronic conductor, as is required by other models. These findings emphasize the importance of incorporation of electrochemical effects at electrode surfaces in interpretation of SP data from geophysical studies. We conclude that SP measurements provide a minimally invasive means for monitoring stimulated sulfate-reduction within saturated sediments.

Introduction

There is growing interest in applying geophysical methods to improve environmental restoration and remediation methodologies. Among such methods, the self-potential (SP) technique has shown promise as an inexpensive yet sensitive means for delineating variations in subsurface geochemical conditions resulting from both abiotic [*Cameron et al.*, 2004; *Corry*, 1985] and biotic processes [*Naudet et al.*, 2003; *Naudet and Revil*, 2005; *Nyquist and Corry*, 2002]. The SP method is a passive technique that measures the open-circuit voltage potential between electrodes located at the ground surface or within boreholes, with the potential-generating mechanism varying according to environmental and measurement conditions. Under conditions where the measurement and reference electrodes are located in geochemically distinct redox environments, self potentials have been shown to be the result of an electrochemical concentration gradient [*Hamilton et al.*, 2004a; b]. In other cases, open-circuit voltages have been attributed to current flow along a conductor, such as ore minerals [*Bigalke and Grabner*, 1997; *Sato and Mooney*, 1960], insoluble metabolic end products [*Naudet and Revil*, 2005], and certain organic polymers [*Naudet et al.*, 2003; *Naudet et al.*, 2004]. The electrical potential distribution associated with electron transfer through conductive media is generally considered to be independent of electrochemical reactions at the electrode surface.

In cases where self-potentials have been attributed to flow through an inert conductor, an alternative hypothesis involving coupling of electrochemical reactions involving the electrode surfaces has been proposed [*Corry*, 1985; *Nyquist and Corry*, 2002]. When bridged through a measuring voltmeter, these authors suggested that electrodes located in the electrochemically distinct regions constitute a galvanic cell, generating a voltage potential that persists as long as the concentration gradient is maintained. Under conditions that lead to the spontaneous flow of current when the two electrodes are connected, electrons will flow from the anode during an oxidation reaction and be transferred to the cathode in a

coupled reduction reaction. Charge balance is maintained via electrolytic conduction through the pore space, which also acts to complete the overall circuit. The electrode composition controls the nature of the half-cell reactions, an effect that should be accounted for when interpreting open-circuit potentials.

The mechanism proposed by Nyquist and Corry can be evaluated by considering the electrode pair in which the measurement (anode) and reference (cathode) electrodes are composed of Ag/AgCl, a non-polarizing electrode design frequently used for SP measurements. When a reduced electroactive species (e.g. HS^-) is present near the anode surface and the cathode is maintained in a more oxidized environment, a voltage potential of ~600-700 mV will result from the coupling of the two half-cell reactions: the oxidation of Ag^0 (as Ag_2S) at the anode and the reduction of AgCl (as Ag^0) at the cathode. Because of the high input impedance of the voltmeter (>10 MΩ), very few electrons are transferred during the measurement process so that electro-active species are not depleted. For anodic reactions that are both thermodynamically and kinetically favorable, such as those occurring between dissolved sulfide and base metals or metal salts, such a galvanic response will dominate the measured SP signal.

Interpreting the self-potential response within the context of a galvanic model makes it possible to use voltage anomalies to monitor chemical changes induced by stimulation of microbial activity. Here we show that the appearance and persistence of aqueous sulfide correlates with the generation of a significant SP voltage and is indicative of microbial sulfate-reduction. Furthermore, spatiotemporal variations in the onset of the SP anomalies closely track the location of active metabolism, reflecting chemotaxis and motility toward elevated substrate concentrations. By interpreting such potentials within the context of predictable and quantifiable galvanic reactions, the SP monitoring approach represents a sensitive and minimally invasive means for detecting the presence of certain electroactive metabolic end products, such as dissolved sulfide.

Methods

We investigated the use of the SP technique for monitoring the onset and location of stimulated sulfate-reduction within saturated sand-packed columns using the sulfate-reducing bacterium, *Desulfovibrio vulgaris*. The experiments were conducted over a period of 40 days using polycarbonate columns having inner diameters of 5.0 cm and lengths of 30.5 cm (Figure 1). Two columns were used: one inoculated and one control column intended to test any abiotic geochemical effects on the SP signals. Fluid samples and SP data were collected on a periodic basis along the length of the column. Upon termination, the inoculated column was destructively evaluated and sediment samples were collected to provide material for electron microscopy.

The columns were packed with silica sand having particle diameters ranging from 600-800 μm and a porosity of 0.37±0.01. The sand was pre-treated with H_2O_2 and a mixture of sodium citrate, $NaHCO_3$, and $Na_2S_2O_4$ to remove any iron oxides before being rinsed, autoclaved, dried, and added to the columns. The columns were then saturated with five pore volumes of de-aired and autoclaved, lactate-deficient feed solution.

The feed solution was designed to resemble sulfate-rich groundwater amended with a source of organic carbon, which had previously been found to support growth of *D. vulgaris*. Final molar concentrations of the primary constituents were as follows: lactate, 3 mM; SO_4^{2-}, 3 mM; Cl^-, 50 mM. No aqueous metals were added to the feed solution in an effort to avoid precipitation of insoluble metal sulfides. The fluid conductivity of the influent solution remained stable over the experimental period at 1950±40 μS/cm. The fluids were rendered anoxic by boiling and cooling under a stream of N_2 and heat sterilized at 121°C for 15min.

Cells of *D. vulgaris* were grown to stationary phase in an enriched (5X) version of the feed solution, centrifuged and rinsed three times, and resuspended in lactate-deficient version, 20 mL of which was

injected into the column via a syringe needle in the vicinity of the electrode located 27 cm from the base of the column (Figure 1). The cells were allowed to affix to the sand grains for 1 day before flow commenced. Lactate-amended fluids were introduced from the bottom using a peristaltic pump. The columns were operated under continuous advective flow having a pore water velocity of 0.50 m d^{-1}. All experiments were conducted within an anaerobic chamber maintained under an atmosphere of N_2/H_2 (95:5).

The SP measurements were made on the inoculated column between four Ag/AgCl electrodes located at 7.0 cm intervals along the column and a single Ag/AgCl reference electrode inserted within the influent flow line (Figure 1). The measurement electrodes were electrically coupled to the sediments via fluid-filled, mesh-capped tubing inserted through the column walls. Measurements were made between the upgradient reference electrode and each of the column-hosted electrodes using a high impedance voltmeter, with the negative lead connected to the reference electrode and the positive lead connected to the measurement electrode. All measurements were made at the same time that fluid samples were obtained. Current flow between the reference and the uppermost electrode was periodically determined by measuring the voltage drop across a known resistance. In an effort to quantify current flow from reference to measurement electrode, current-voltage and current-power relationships for the electrode pair were generated by varying the resistor values between 1 MΩ and 400 Ω.

Solution samples from the influent, effluent, and multi-port samplers were analyzed for lactate, SO_4^{2-}, and total S^{2-} at 1-5 day intervals over the experimental period. The multi-port samplers were spaced at 7.0 cm intervals along the inoculated column, with positions opposite from each of the SP electrodes. The concentration of lactate and SO_4^{2-} was determined by gradient elution ion-chromatography, while total S^{2-} concentration was determined colorimetrically [*Cline*, 1969]. Cell densities were determined using quantitative live/dead staining [*Levin et al.*, 1992] for each sampling location at six time points during the experiment (day 2, 12, 19, 29, and 35).

Another column of similar design was used to isolate the SP-generating mechanism in the absence of microbial activity. This column was not operated under advective flow conditions; rather a fluid reservoir containing a solution of known sulfide concentration was connected to the top of the sediment column (Figure 1). After filling the reservoir with a fluid identical in composition to that used to saturate the sediments, an appropriate volume of 1 M Na_2S was added to the reservoir to adjust the sulfide concentration to a desired value and the system allowed to equilibrate under static conditions for 2 hours. The pH of the reservoir solution was measured and adjusted to a value of 7.5 through the addition of an appropriate buffer (1 N HCl or NaOH). A sulfide-dependent SP response curve was generated by iteratively increasing the sulfide concentration from 0.01 to 4 mM and measuring the SP response between the reference electrode and an Ag/AgCl electrode coupled to the reservoir.

Post-experimental analysis provided samples for characterizing the extent to which the grain surfaces were coated and pores filled by microbial biomass, extracellular polymers, and mineral precipitates that could contribute to the SP response by providing a conductive pathway. Samples for scanning electron microscopy (SEM) analysis were collected at 4.0 cm intervals along the inoculated column, immersed overnight in a 2.5% solution of glutaraldehyde, rinsed three times, dehydrated in an ethanol series, and dried in a critical point drying unit. Samples were extruded onto carbon-coated stubs, sputter-coated with carbon, and analyzed using a Philips XL30 SEM. All samples were preserved anaerobically until the time of analysis.

Results

The influent solution concentrations of lactate, SO_4^{2-}, and Cl^- for both columns remained constant over the 40-day experiment, with variations never exceeding ±2% of their initial value. In contrast, concentrations of lactate and SO_4^{2-} near the point of inoculation (27.0 cm from the inlet) decreased dramatically after 2-3 days. Lactate concentrations at this location fell from influent values of 3 mM to

levels below detection (data not shown) and remained depleted for the duration of the experiment. A concomitant decrease in the SO_4^{2-} concentration at this location was accompanied by an increase in total dissolved sulfide (Figure 2). After the initial decrease, sulfate and sulfide remained at quasi steady-state levels of 1.3 mM and 0.8 mM, respectively. This represents a decrease in sulfate concentration of 1.7 mM, yielding a consumption rate of 0.4 mmol kg^{-1} day^{-1}. After the onset of sulfate-reduction, the effluent pH increased from an initial value of 7.2 to relatively constant value of 7.5±0.15.

Analysis of solution samples taken from the multi-port samplers on the inoculated column indicated that the location of sulfide production shifted downward with time (i.e. toward the point of nutrient influx). There was an iterative decrease in the SO_4^{2-} concentration with time at four locations along the column, accompanied by an increase in total sulfide (Fig. 2). In the absence of aqueous or sorbed metals, no visible mineral precipitates formed within the inoculated column following the production of aqueous sulfide. The amounts of dissolved sulfide produced were stoichiometrically similar to the amount of sulfate consumed, as expected given the absence of complexing metals in the experiments. The influent fluids were compositionally identical for both inoculated and control columns, and no significant change in the effluent concentrations of lactate, SO_4^{2-}, or total sulfide was observed for the control column (data not shown).

The concentration of planktonic cells along the inoculated column shifted downward with time, most likely the result of chemotaxis towards the region of greatest substrate concentration. Cell concentrations ranged from 10^3 to 10^5 cells/mL on day 2, with the highest concentrations near the point of inoculation. These values increased by nearly two orders of magnitude by day 12 and the greatest increases were for the two furthest downgradient locations. From day 19 through the end of the experiment, the greatest increases in cell concentration occurred closer to the base, from 4 to 12 cm. Although downgradient concentrations decreased with time after day 19, they remained elevated by at least two orders of magnitude over baseline levels.

For each of the four electrode locations, the open-circuit potential (SP voltage) showed a pronounced increase in magnitude following the onset of sulfate-reduction in the vicinity of the measurement electrode. The anomalous voltages initially occurred near the point of inoculation, migrating downwards toward the point of nutrient influx with time (Figure 2) in a manner consistent with the transient geochemical and microbial fronts. At all locations, the onset of the SP anomaly coincided with the depletion of lactate and sulfate and the increase in dissolved sulfide, and resulted in a typical open-circuit potential of –640 to –690 mV (negative values are the result of connecting the negative lead to the reference electrode, as is the convention for self-potential measurements). In advance of microbial activity, no anomalous SP signatures were observed for any of the electrode locations in the inoculated column. Rather, the open-circuit potential remained close to background levels for each, having a value of –15±5 mV. Additionally, there was no measurable difference in the SP voltage measured under flow or no-flow conditions.

In contrast to the uninoculated control column where none of the four electrode locations showed significant variation over the 40-day experiment (data not shown), the presence of dissolved sulfide in the vicinity of a measurement electrode in the inoculated column led to an immediate response in the SP signature. By day 40, the open circuit potentials measured between the reference and four downgradient electrodes returned to baseline levels as the dissolved sulfide concentration reached a uniform value along the column flowpath. While not directly measured, the presence of dissolved sulfide in the vicinity of the reference electrode was inferred due to a visible darkening of the electrode surface, which corresponded in time to the sudden disappearance of the downgradient SP anomalies.

Current flow between the reference electrode and the 27 cm location was monitored before, during, and after development of the SP anomaly in order to generate the current-voltage and current-power relationships for the electrode pair. While there was no measurable current flow either before the development of the SP anomaly or after its disappearance, when measured 10 days into the experiment,

current flow and resultant power production were significant (Figure 3). As the resistance was lowered in a step-wise fashion, current flow increased from 0.663 μA at 1 MΩ to 17.5 μA at 400 Ω, with a concomitant decrease in the voltage from 663 mV to 7 mV. When normalized to the surface area of the measurement electrode, the resulting current densities ranged from 1.0 to 27.5 $\mu A/cm^2$. Power production between the electrodes showed a parabolic trend reaching a maximum value of 3.2 μW or 4.9 $\mu W/cm^2$.

In order to test the relative importance of microbial versus geochemical SP source-generating mechanisms, a series of self-potential, current-voltage, and current-power measurements were made using the static, abiotic sulfide-amended column design. As the sulfide concentration within the fluid reservoir was increased from 0.01 to 4 mM, the absolute magnitude of the SP voltage measured between the reference and measurement electrode increased from 395 to 724 mV, respectively (Figure 4). The SP response increased logarithmically for sulfide concentrations between 0.01 and 0.04 mM before increasing linearly from 0.04 to 4 mM. Also shown in Figure 4 is the theoretical electrochemical cell potential for the proposed galvanic cell at pH 7.5 and as a function of HS^- concentration. There is a strong correlation between the measured SP voltage and the predicted electrochemical cell potential for sulfide concentrations greater than ~0.04 mM. Below this threshold concentration, the theoretical cell potential greatly over predicted the measured SP response. Whether this was the result of diffusional or kinetic constraints or the presence of a competing anodic half-reaction was not determined. The current-voltage and current-power relationships for the abiotic configuration were determined for the 1 mM sulfide concentration, with the results obtained over the same range of resistance values closely matching those shown in Figure 3 within ±1% (data not shown), confirming the transfer of electrons from anode to cathode upon completion of the circuit.

Destructive sampling of the inoculated column sediments and analysis using SEM revealed extensive biofilm formation (Figure 5), particularly towards the influent end and in the vicinity of the 6 cm

electrode location. Although the precise hydrated geometry of the biofilm was undoubtedly altered during sample preparation, numerous organic polymers were observed to link individual cells, which were widely dispersed throughout the pore network. Analysis of backscattered electrons from these samples failed to reveal regions of high electron-density (data not shown), corroborating the lack of any visible sulfide mineral precipitation within the pore space.

Discussion

Anomalous open-circuit potentials (i.e., the SP voltages) correlate well with the accumulation of dissolved sulfide within pores, suggesting the utility of the SP method for monitoring stimulated sulfate-reduction. Precipitation of mineral phases in pore spaces was prevented in the experiment because soluble metals were excluded from the saturating fluid and metal oxides were removed from the sediments via chemical extraction. Consequently, no inert conductor existed that could bridge electrochemically distinct regions, thereby transferring electrons from reduced to oxidized locations. For the conditions studied here, our observations render the often-cited SP source generating mechanism that relies on the transfer of electrons through an inert conductor [*Sato and Mooney*, 1960; *Sivenas and Beales*, 1982] highly implausible. Similarly, dissipation of the voltage anomaly despite persistence of biofilms and cell-bridging organic polymers [*Naudet et al.*, 2003; *Naudet and Revil*, 2005] indicates that polymers were not responsible for electron flow that caused the SP signal. Although we accept that current flow can occur through polymers [*Gorby et al.*, 2006; *Reguera et al.*, 2005; *Reguera et al.*, 2006], the magnitude was not sufficient to sustain a measurable SP anomaly under the conditions of our experiment.

Because no endogenous current flow was required within the system in order to generate the measured SP response, we consider an alternative explanation in which the SP response was dominated by differences in the reduction potential between the reference and measurement electrodes. This

explanation may be generally applicable in cases where the measurement electrode surface was deliberately or inadvertently exposed to the geochemical surroundings. In contrast, this explanation may be inadequate to fully explain SP anomalies attributed to variations in subsurface redox conditions, such as those reported by *Naudet et al.* [2003], where no difference exists in the geochemical conditions immediately surrounding the electrode locations.

Evidence in support of a galvanic mechanism underlying the SP response comes from the current-voltage and current-power relationships obtained during the experiment. If the transfer of electrons from reduced to oxidized locations via an inert internal conductor was the dominant source of the SP response, current flow through the circuit created by connection of the measurement and reference electrodes would be negligible. In contrast, we observed significant electron flow through this external circuit, which exhibited current- and power-densities that are in excellent agreement with reported sulfide-dependent galvanic fuel cells [*Rabaey et al.*, 2006; *Reimers et al.*, 2006; *Tender et al.*, 2002]. This observation was corroborated by the abiotic experiment and confirms that electron transfer through biogenic materials [*Naudet et al.*, 2003; *Naudet and Revil*, 2005] can be neglected as an alternate source for the SP voltage anomalies observed here.

Previous studies have shown a positive correlation between anomalous self-potentials and reducing conditions [*Naudet et al.*, 2003; *Naudet et al.*, 2004; *Naudet and Revil*, 2005; *Nyquist and Corry*, 2002; *Timm and Moller*, 2001]. However, where applicable, relatively few authors have implicated the immediate geochemical environment of the reference and measurement electrodes as the dominant factor in generating an SP response [*Corry*, 1985; *Nyquist and Corry*, 2002]. Under our experimental conditions, the results support the contention that electrochemical interactions between the electrode surface and the surrounding environment can generate a significant SP response, even for cases in which non-polarizing electrodes are used. We attribute these anomalies to electrochemical concentration gradients between sulfide-rich regions and areas having higher oxidation potential. When the

measurement and reference electrodes - both Ag/AgCl - were bridged through a voltmeter, a spontaneous galvanic cell was created in which oxidation of Ag^0 to Ag_2S at the anode could be coupled to the reduction of Ag^+ to Ag^0 at the cathode, with the intervening saturated sediments acting as the salt bridge necessary for charge conservation and completion of the circuit. With the electrodes thus configured, the reduction potential for the two half-cell reactions may be calculated, corrected for concentration-specific effects via the Nernst equation, and subtracted to yield the overall cell potential for the galvanic pair; this theoretical cell potential may then be compared to the observed SP anomalies.

In the case of the anodic half-cell reaction, a two-step process likely occurs at the electrode-fluid interface. First, conversion of AgCl to Ag_2S in the presence of bisulfide (HS^-) results from the large difference in solubility products between Ag_2S and AgCl, with values of $K_{sp}=10^{-51}$ and 10^{-10}, respectively:

$$AgCl_{(s)} + HS^-_{(aq)} \rightarrow Ag_2S_{(s)} + Cl^-_{(aq)} \qquad (1)$$

strongly favoring the formation of Ag_2S. The result is the creation of a Ag/Ag_2S electrode having a standard reduction potential equivalent to that shown in (2). Subsequently, and as a result of the semi-porous nature of the AgCl coating, the Ag^0 core of the Ag/AgCl electrode may react directly to form Ag_2S in the presence of HS^-, the dominant sulfide species under the pH conditions of the experiment:

$$Ag_2S_{(s)} + H^+ + 2e^- \rightarrow 2Ag^0_{(s)} + HS^-_{(aq)} \qquad E^0 = -0.273 \text{ V} \qquad (2)$$

In the absence of dissolved sulfide, the cathodic half-cell reaction is simply that of the standard Ag/AgCl reference electrode, here written as a reduction reaction:

$$AgCl_{(s)} + 1e^- \rightarrow Ag^0_{(s)} + Cl^-_{(aq)} \qquad E^0 = 0.220\ V \qquad (3)$$

Combining equations (2) and (3) yields the coupled overall reaction, which constitutes the galvanic cell created by bridging the measurement and reference electrodes through the voltmeter:

$$2AgCl_{(s)} + HS^-_{(aq)} \rightarrow Ag_2S_{(s)} + H^+ + 2Cl^-_{(aq)} \qquad (4)$$

The reaction shown in (4) has a standard cell potential calculated as the difference between the cathodic and anodic half-cell reduction potentials at standard-state conditions:

$$\Delta E^0 = E^0\ (\text{cathode}) - E^0\ (\text{anode}) = 0.493\ V \qquad (5)$$

When experiment-relevant values for pH (7.5) and [Cl^-] (50 mM) are considered, the Nernst equation at 25°C yields a [HS^-]-dependent value for ΔE, which is shown in Figure 4 and given as:

$$\Delta E = \Delta E^0 - \frac{0.0592\text{V}}{\text{n}} \log \frac{[\text{H}^+]\,[\text{Cl}^-]^2}{[\text{HS}^-]} \qquad (6)$$

where n, the number of electrons transferred per mole of HS^- reacted, is 2.

Abiotic experiments in which sulfide concentration gradients were systematically varied showed a positive correlation between the magnitude of the measured SP anomaly and the theoretical cell potential (Figure 4), particularly for $[HS^-]$ in excess of 40 μM. In environments where sulfate-reduction is a dominant metabolic process, dissolved sulfide concentrations are typically well in excess of this value. Given $[HS^-]$ values observed in the biological portion of our experiment (750-900 μM), equation (6) yields a theoretical cell potential of 700-703 mV, in close agreement with the anomalous SP voltages measured.

As dissolved sulfide became homogenously distributed throughout the column in our experiment, including in the region of the reference electrode, the difference in the reduction potential between the measurement and reference electrodes vanished, as did the measured open-circuit voltage at all four electrode locations. This is as expected, given that geochemical equilibration of the measurement and reference electrode locations will ultimately eliminate the electrochemical driving force behind the SP response.

Our studies suggest that, under ideal conditions, the absolute magnitude of the SP response should be indicative of the $[HS^-]$ concentration surrounding the measurement electrode. In many respects, this is analogous to an ion-selective electrode-based analysis of the concentration of a chemical species such as sulfide, but deployed at the column and potentially the field-scales. In contrast to a laboratory setting, incomplete understanding of the geochemical conditions surrounding the reference electrode, poor electrode coupling, and the presence of competing half-cell reactions in a field application may prevent

quantification of the dissolved sulfide concentration from the SP value. However, given the use of either metal (e.g. Cu^0 or Pb^0) or metal-salt electrodes (e.g. Ag/AgCl or $Pb/PbCl_2$), the presence of dissolved sulfide in the vicinity of the measurement electrode should yield a voltage anomaly diagnostic of sulfate-reduction.

The sign of the value of SP anomaly should provide information about the geochemical conditions at the measurement electrodes. In our experiments, the negative anomalies agree with predictions of the galvanic model. Per the traditional SP measurement convention, the negative and positive leads of the voltmeter were attached to the reference and measurement electrodes, respectively. Under conditions where the reduction potential is lower at the measurement electrode than at the reference electrode, the measurement electrode will constitute the anode - the site where electrons are derived through an oxidative process. By connecting the positive lead of the voltmeter to the anodic electrode, one would expect to measure a negative potential, just as one observes when the polarity is reversed when measuring the voltage of a battery. Consequently, the sign of the measured anomaly will be diagnostic of whether anodic or cathodic processes are occurring at the measurement and reference electrode locations.

In addition to localizing zones of redox disequilibria and providing information about their spatial arrangement, the SP measurements may be used to track motility of microorganisms that generate redox-active byproducts (e.g., sulfide and ferrous iron). Microbial sulfate-reduction initiated in zones with the highest cell concentrations (near the point of inoculation at 27 cm) and generated an SP value of –690 mV. Voltage anomalies of similar magnitude were detected at progressively later times along the length of the column in the direction of nutrient influx. The spatiotemporal changes in both solute and planktonic cell concentrations indicated chemotaxis by *D. vulgaris* toward the region of greatest substrate concentration [*Johnson et al.*, 1997]. Although the direction of cell migration was against flow, fluid flux near the grain boundaries was sufficiently low to allow for upgradient motility, consistent with previous

observations [*Williams et al.*, 2005]. Using the initial appearance of an anomalous SP voltage at a given electrode location and the time interval between the SP response, the rate of motility within the sediments was determined to be between 0.4 and 0.5 m/day, in close agreement with other studies of microbial motility in saturated porous media [*Witt et al.*, 1999].

Conclusions

Here we have shown that the stimulation of sulfate-reducing microorganisms and the accumulation of dissolved sulfide near the electrode surface create electrochemical changes that are directly detectable using the self-potential geophysical technique. We have resolved spatiotemporal changes in open-circuit potentials resulting from variations in the onset and location of sulfate-reduction, allowing for the tracking of microbial motility accompanying chemotaxis within saturated sediments. So long as elevated sulfide-concentrations were confined exclusively to measurement electrode locations, the anomalous SP voltages persisted over time, providing an indirect indication of sustained metabolic activity. Our laboratory results are relevant to the larger spatial scales of the natural environment where methods currently used for field-scale self-potential monitoring may be used in an analogous fashion. The approach may be applied in a variety of natural systems, particularly where there are no large concentrations of metals that would sequester sulfide into conductive mineral precipitates and when no abiotic oxidants (e.g., dissolved oxygen or structural ferric iron) are available to reoxidize the dissolved sulfide. As the role of sulfate-reducing bacteria in the precipitation of toxic metals is well documented and strategies involving their stimulation are currently under investigation for the field scale remediation of contaminated sites [*Smith and Gadd*, 2000; *White and Gadd*, 1996], our results show the potential of using galvanic techniques for efficiently monitoring regions of stimulated sulfate-reduction and for evaluating the sustenance of redox conditions favorable for the long-term stability of reduced precipitates.

Acknowledgments. Funding for this study was provided by the Environmental Remediation Science Program, Office of Biological and Environmental Research, U.S. Department of Energy (DOE) (Grant DE-AC03-76SF00098). Electron microscopy was carried out in the Environmental Molecular Sciences Laboratory, a national scientific user facility sponsored by DOE's Office of Biological and Environmental Research and located at Pacific Northwest National Laboratory. We thank Bruce Arey for his assistance in preparing and analyzing the SEM samples.

References

Bigalke, J., and E. W. Grabner (1997), The geobattery model: A contribution to large scale electrochemistry, *Electrochim. Acta*, *42*(23-24), 3443-3452.

Cameron, E. M., S. M. Hamilton, M. I. Leybourne, G. E. M. Hall, and M. B. McClenaghan (2004), Finding deeply buried deposits using geochemistry, *Geochem-Explor. Env. A*, *4*, 7-32.

Cline, J. D. (1969), Spectrophotometric determination of hydrogen sulfide in natural waters, *Limnol. Oceanogr.*, *14*(3), 454-458.

Corry, C. E. (1985), Spontaneous polarization associated with porphyry sulfide mineralization, *Geophysics*, *50*(6), 1020-1034.

Gorby, Y. A., et al. (2006), Electrically conductive bacterial nanowires produced by Shewanella oneidensis strain MR-1 and other microorganisms, *P. Natl. Acad. Sci. USA*, *103*(30), 11358-11363.

Hamilton, S. M., E. M. Cameron, M. B. McClenaghan, and G. E. M. Hall (2004a), Redox, pH and SP variation over mineralization in thick glacial overburden. Part I: Methodologies and field investigation at the Marsh Zone gold property, *Geochem-Explor. Env. A*, *4*, 33-44.

Hamilton, S. M., E. M. Cameron, M. B. McClenaghan, and G. E. M. Hall (2004b), Redox, pH and SP variation over mineralization in thick glacial overburden. Part II: Field investigation at Cross Lake VMS property, *Geochem-Explor. Env. A*, *4*, 45-58.

Johnson, M. S., I. G. Zhulin, M. E. R. Gapuzan, and B. L. Taylor (1997), Oxygen-dependent growth of the obligate anaerobe Desulfovibrio vulgaris Hildenborough, *J. Bacteriol.*, *179*(17), 5598-5601.

Levin, M. A., R. J. Seidler, and M. Rogul (1992), *Microbial ecology: Principles, methods, and applications*, 945 pp., McGraw-Hill, New York.

Naudet, V., A. Revil, J. Y. Bottero, and P. Begassat (2003), Relationship between self-potential (SP) signals and redox conditions in contaminated groundwater, *Geophys. Res. Lett.*, *30*(21), 2091, doi:10.1029/2003GL018096.

Naudet, V., A. Revil, E. Rizzo, J. Y. Bottero, and P. Begassat (2004), Groundwater redox conditions and conductivity in a contaminant plume from geoelectrical investigations, *Hydrol. Earth Syst. Sc.*, *8*(1), 8-22.

Naudet, V., and A. Revil (2005), A sandbox experiment to investigate bacteria-mediated redox processes on self-potential signals, *Geophys. Res. Lett.*, *32*, L11405, doi:10.1029/2005GL022735.

Nyquist, J. E., and C. E. Corry (2002), Self-potential: The ugly duckling of environmental geophysics, *Leading Edge of Geophysics*, *21*(5), 446-451.

Rabaey, K., et al. (2006), Microbial fuel cells for sulfide removal, *Environ. Sci. Technol.*, *40*(17), 5218-5224.

Reguera, G., K. D. McCarthy, T. Mehta, J. S. Nicoll, M. T. Tuominen, and D. R. Lovley (2005), Extracellular electron transfer via microbial nanowires, *Nature*, *435*(7045), 1098-1101.

Reguera, G., K. P. Nevin, J. S. Nicoll, S. F. Covalla, T. L. Woodard, and D. R. Lovley (2006), Biofilm and nanowire production leads to increased current in Geobacter sulfurreducens fuel cells, *Appl. Environ. Microb.*, *72*(11), 7345-7348.

Reimers, C. E., P. Girguis, H. A. S. III, L. M. Tender, N. Ryckelynck, and P. Whaling (2006), Microbial fuel cell energy from an ocean cold seep, *Geobiology*, *4*, 123-136.

Sato, M., and H. M. Mooney (1960), The electrochemical mechanism of sulfide self-potentials, *Geophysics*, *25*, 226-249.

Sivenas, P., and F. W. Beales (1982), Natural geobatteries associated with sulfide ore-deposits, 1. Theoretical-studies, *J. Geochem. Explor.*, *17*(2), 123-143.

Smith, W. L., and G. M. Gadd (2000), Reduction and precipitation of chromate by mixed culture sulphate-reducing bacterial biofilms, *Journal of Applied Microbiology*, *88*(6), 983-991.

Tender, L. M., C. E. Reimers, H. A. Stecher, D. E. Holmes, D. R. Bond, D. A. Lowy, K. Pilobello, S. J. Fertig, and D. R. Lovley (2002), Harnessing microbially generated power on the seafloor, *Nat. Biotechnol.*, *20*(8), 821-825.

Timm, F., and P. Moller (2001), The relation between electric and redox potential: Evidence from laboratory and field measurements, *J. Geochem. Explor.*, *72*(2), 115-128.

White, C., and G. M. Gadd (1996), Mixed sulphate-reducing bacterial cultures for bioprecipitation of toxic metals: Factorial and response-surface analysis of the effects of dilution rate, sulphate and substrate concentration, *Microbiol.*, *142*, 2197-2205.

Williams, K. H., D. Ntarlagiannis, L. D. Slater, A. Dohnalkova, S. S. Hubbard, and J. F. Banfield (2005), Geophysical imaging of stimulated microbial biomineralization, *Environ. Sci. Technol.*, *39*(19), 7592-7600.

Witt, M. E., M. J. Dybas, R. M. Worden, and C. S. Criddle (1999), Motility-enhanced bioremediation of carbon tetrachloride-contaminated aquifer sediments, *Environ. Sci. Technol.*, *33*(17), 2958-2964.

Figure 1. Column design illustrating the location of (a) the saturated sand pack and fluid flow direction, (b) the measurement and (c) reference Ag/AgCl electrode locations, and (d) the reservoir chamber used for the abiotic sulfide-amendment test, which replaced the end-cap apparatus (e) used during the continuous-flow biostimulation experiment. Flow through the column was from bottom to top. The electrodes were spaced at 7.0 cm intervals, with the distances noted measured from the base of the column; fluid sampling ports (not shown) were located directly opposite each electrode.

Figure 2. Inoculated column solution chemistry and SP response during the stimulation of *D. vulgaris*; sulfate (filled square), total sulfide (open square), and SP in mV (open circle); chemical concentrations and SP voltages are plotted on the right- and left-hand axes, respectively. Data from the four locations are shown as labeled, with distances measured from the base of the column.

Figure 3. Current-voltage (filled square) and current-power (open square) relationships for the inoculated column on day 10 of the experiment. Current flow was determined by connecting the reference and uppermost measurement electrode through a resistor of known value; total current flow and power production were then determined by iteratively lowering resistance of the circuit.

Figure 4. SP voltages as a function of sulfide concentration using the abiotic column design. The cell potential as a function of $[HS^-]$ (bold line), measured SP voltage (absolute value; filled circles) and theoretical cell potential (open squares) at six discrete sulfide concentrations. The theoretical cell potentials were determined over the $[HS^-]$ range indicated, while holding $[Cl^-]$ (50 mM) and pH (7.5) constant.

Figure 5. SEM image of cells recovered from the base of the column illustrating the dense network of cell-bridging organic polymers present within the biofilm structure.

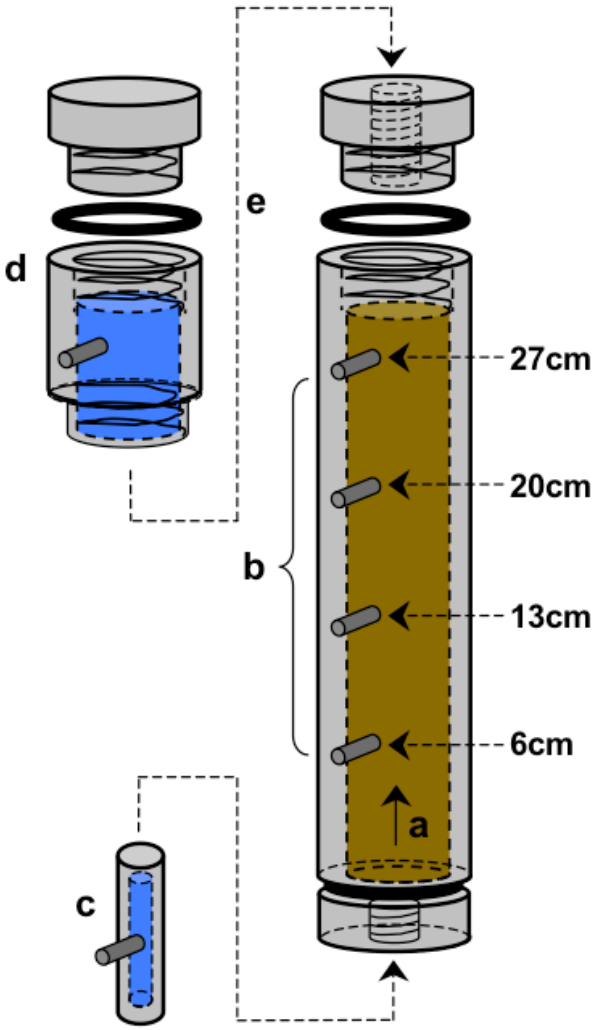

Figure 1. Column design illustrating the location of (a) the saturated sand pack and fluid flow direction, (b) the measurement and (c) reference Ag/AgCl electrode locations, and (d) the reservoir chamber used for the abiotic sulfide-amendment test, which replaced the end-cap apparatus (e) used during the continuous-flow biostimulation experiment. Flow through the column was from bottom to top. The electrodes were spaced at 7.0 cm intervals, with the distances noted measured from the base of the column; fluid sampling ports (not shown) were located directly opposite each electrode.

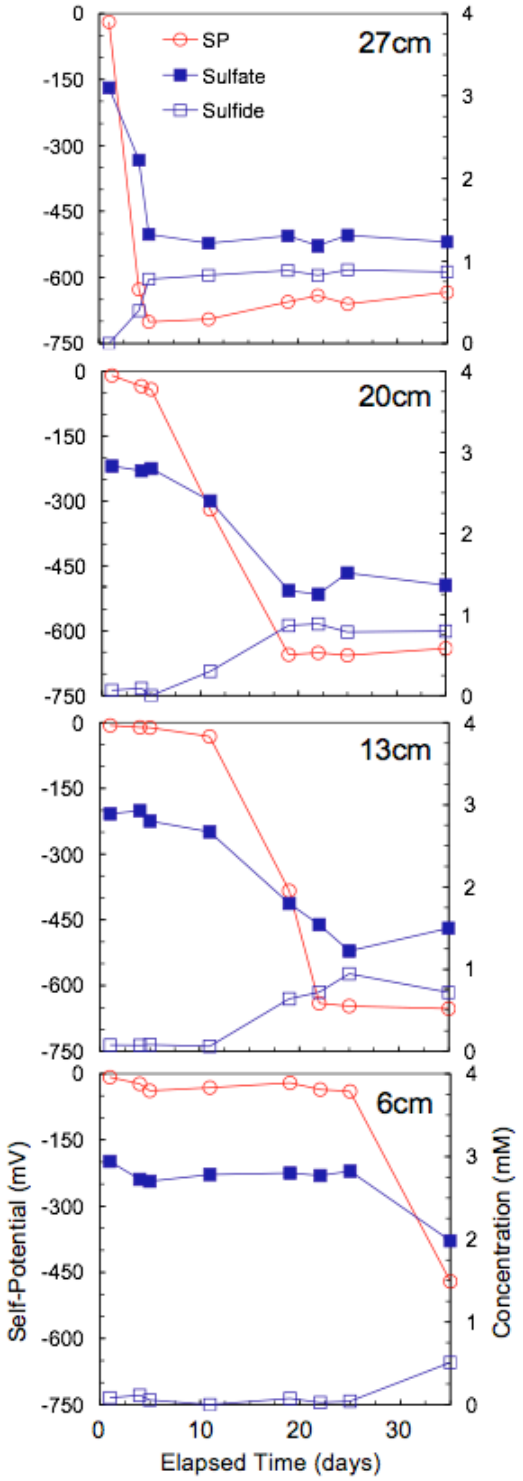

Figure 2. Inoculated column solution chemistry and SP response during the stimulation of *D. vulgaris*; sulfate (filled square), total sulfide (open square), and SP in mV (open circle); chemical concentrations and SP voltages are plotted on the right- and left-hand axes, respectively. Data from the four locations are shown as labeled, with distances measured from the base of the column.

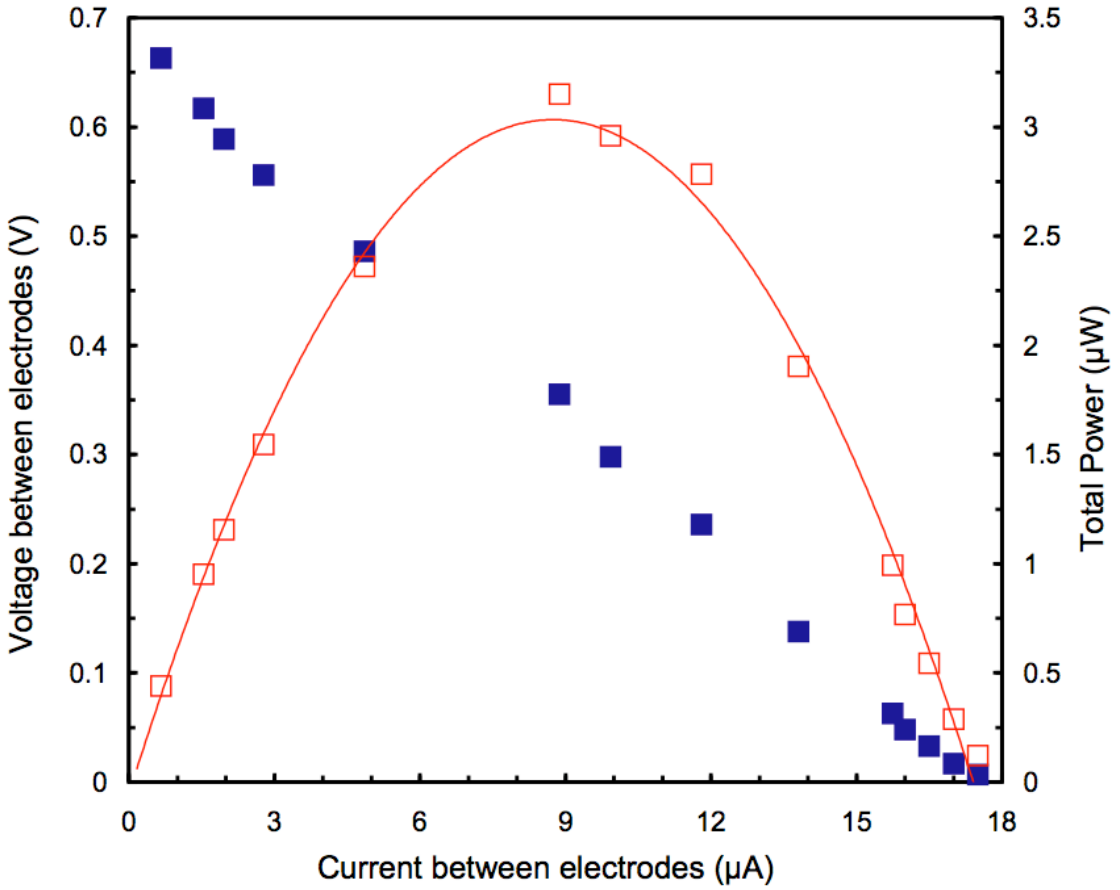

Figure 3. Current-voltage (filled square) and current-power (open square) relationships for the inoculated column on day 10 of the experiment. Current flow was determined by connecting the reference and uppermost measurement electrode through a resistor of known value; total current flow and power production were then determined by iteratively lowering resistance of the circuit.

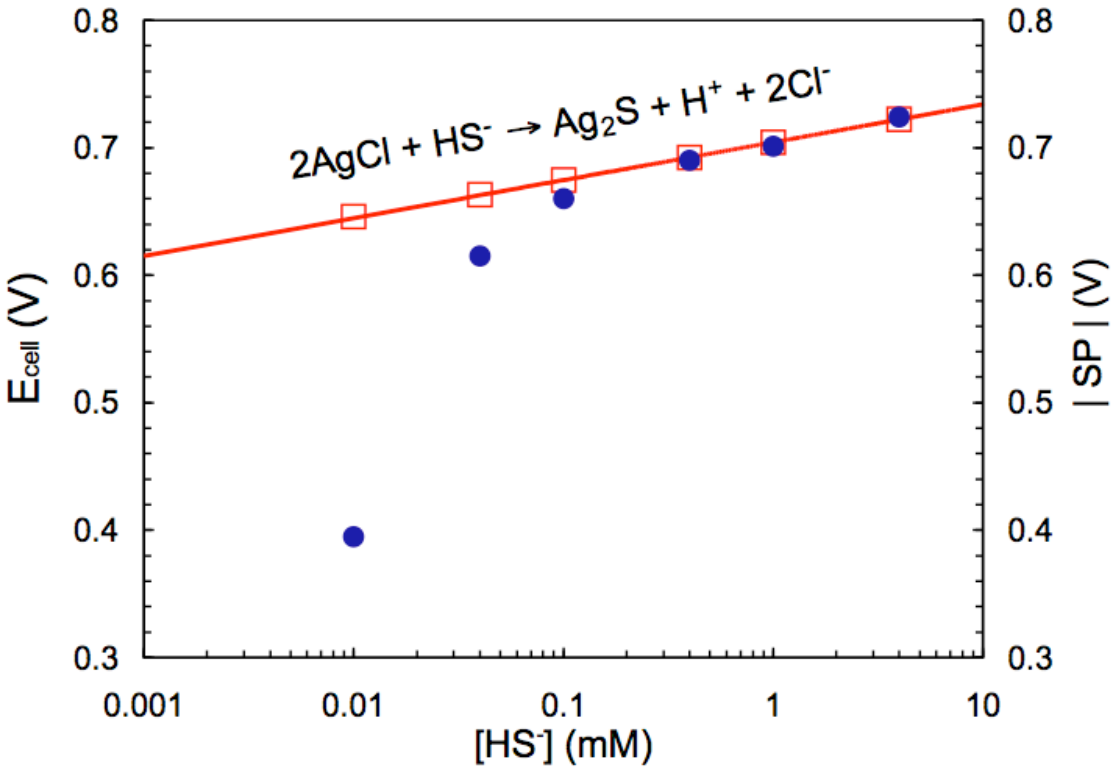

Figure 4. SP voltages as a function of sulfide concentration using the abiotic column design. The cell potential as a function of [HS^-] (bold line), measured SP voltage (absolute value; filled circles) and theoretical cell potential (open squares) at six discrete sulfide concentrations. The theoretical cell potentials were determined over the [HS^-] range indicated, while holding [Cl^-] (50 mM) and pH (7.5) constant.

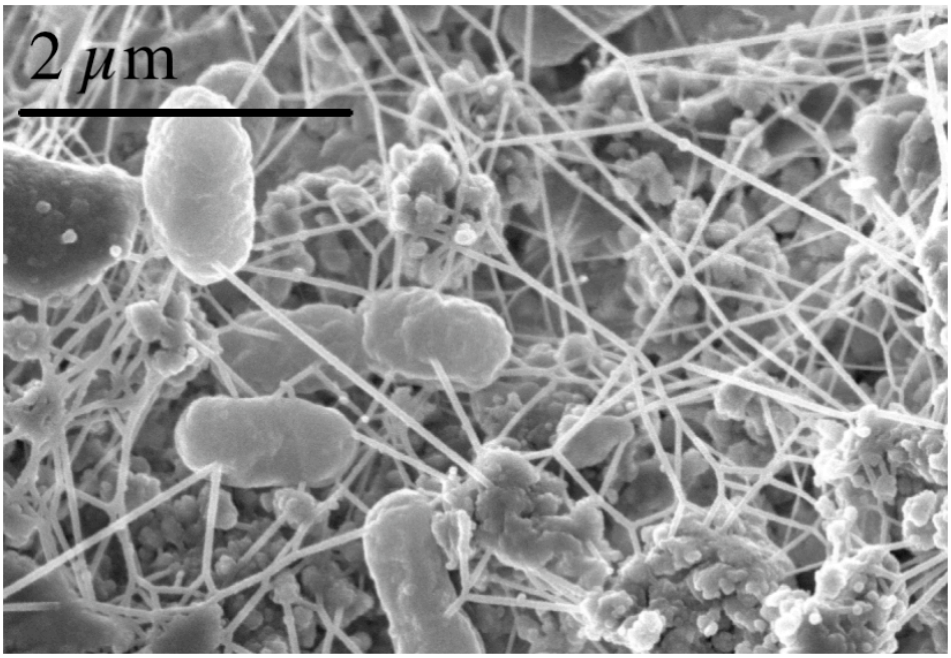

Figure 5. SEM image of cells recovered from the base of the column illustrating the dense network of cell-bridging organic polymers present within the biofilm structure.